PHYSICAL REVIEW B **86**, 195131 (2012)

Spin-orbit coupling in iridium-based 5*d* compounds probed by x-ray absorption spectroscopy

J. P. Clancy,[1] N. Chen,[2] C. Y. Kim,[2] W. F. Chen,[2] K. W. Plumb,[1] B. C. Jeon,[3] T. W. Noh,[3] and Young-June Kim[1]
[1]*Department of Physics, University of Toronto, Toronto, Ontario, M5S 1A7, Canada*
[2]*Canadian Light Source, Saskatoon, Saskatchewan, S7N 0X4, Canada*
[3]*ReCFI, Department of Physics and Astronomy, Seoul National University, Seoul 151-747, Korea*

(Received 30 May 2012; revised manuscript received 29 September 2012; published 19 November 2012)

We have performed x-ray absorption spectroscopy (XAS) measurements on a series of Ir-based 5*d* transition metal compounds, including Ir, $IrCl_3$, IrO_2, Na_2IrO_3, Sr_2IrO_4, and $Y_2Ir_2O_7$. By comparing the intensity of the "white-line" features observed at the Ir L_2 and L_3 absorption edges, it is possible to extract valuable information about the strength of the spin-orbit coupling in these systems. We observe remarkably large, nonstatistical branching ratios in all Ir compounds studied, with little or no dependence on chemical composition, crystal structure, or electronic state. This result confirms the presence of strong spin-orbit coupling effects in novel iridates such as Sr_2IrO_4, Na_2IrO_3, and $Y_2Ir_2O_7$, and suggests that even simple Ir-based compounds such as IrO_2 and $IrCl_3$ may warrant further study. In contrast, XAS measurements on Re-based 5*d* compounds, such as Re, ReO_2, ReO_3, and Ba_2FeReO_6, reveal statistical branching ratios indicative of negligible spin-orbit coupling effects.

DOI: 10.1103/PhysRevB.86.195131 PACS number(s): 71.70.Ej, 78.70.Dm, 71.20.−b, 75.50.−y

I. INTRODUCTION

In recent years there has been growing interest in the physics of materials based on 5*d* transition metal elements.[1–27] Due to the broad, spatially extended nature of 5*d* electronic wave functions, these materials tend to exhibit wide electronic bands, with relatively weak electronic correlations (U $\sim$ 0.5–3 eV) and strong crystal field effects (CF $\sim$ 1–5 eV). Furthermore, because of the large atomic mass associated with 5*d* elements, these materials also tend to exhibit strong relativistic spin-orbit coupling effects (SO $\sim$ 0.1–1 eV). The close correspondence of these three energy scales (U $\approx$ CF $\approx$ SO) presents an extremely promising opportunity for the study of physics arising from competing spin, orbital, charge, and lattice degrees of freedom.

One family of 5*d* compounds which have begun to attract particular experimental and theoretical attention are the iridium-based transition metal oxides, or iridates.[1–27] The majority of these compounds are based on Ir^{4+} ions, which display a $5d^5$ electronic configuration. One of the fundamental puzzles surrounding these materials is that in spite of the fact that simple band theory arguments suggest they should be metallic, a surprising number of iridates appear to be insulators.[3,4,11,12,21] This result is particularly remarkable since the relatively weak 5*d* electron-electron correlations are too small to drive a conventional Mott insulator transition (as in many 3*d* transition metal oxide systems). Instead, this phenomena has been attributed to the presence of much stronger 5*d* spin-orbit coupling effects, which can be combined with the modest electronic correlations to produce a novel "spin-orbital Mott insulator" with a $j_{\text{eff}} = 1/2$ ground state.[1,2]

Among the iridates that have attracted the most significant recent attention are Sr_2IrO_4,[1–10] Na_2IrO_3,[12–18] and $Y_2Ir_2O_7$.[21–27] Sr_2IrO_4 is a layered perovskite compound with a structure similar to the parent compound of the high T_c cuprates La_2CuO_4.[5,6] This compound develops canted antiferromagnetic order below $T_N \sim 240$ K,[2] and has been reported to display unusually large magnetoelastic[7] and magnetoelectric effects.[8] More importantly, however, Sr_2IrO_4 is notable for being the first proposed experimental realization of a $j_{\text{eff}} = 1/2$ spin-orbital Mott insulator.[1,2] Na_2IrO_3 is a honeycomb lattice material, which has attracted considerable interest due to its potential relevance to the Kitaev-Heisenberg model.[13–17] This model, which describes a system of $S = 1/2$ moments on a honeycomb lattice with highly anisotropic exchange interactions, has been proposed to exhibit novel spin liquid and topologically ordered states.[17] $Y_2Ir_2O_7$ is a pyrochlore iridate, with a structure composed of Ir ions distributed on a network of corner-sharing tetrahedra. This crystal structure gives rise to a natural tendency towards geometric frustration, and members of the $R_2Ir_2O_7$ series (R = lanthanide) have been associated with exotic spin liquid and spin ice states.[19,20] $Y_2Ir_2O_7$, in particular, has also been put forward as a potential topological insulator or topological (Weyl) semimetal.[23–27] Although the detailed physics of these three systems vary significantly, in all three cases it is the presence of strong 5*d* spin-orbit coupling effects that is believed to drive the development of unconventional electronic and magnetic ground states.

Given the apparent importance of spin-orbit coupling effects in the iridates, it is natural to attempt to quantify the strength of the spin-orbit interactions in these compounds. One method of accomplishing this is provided by the technique of x-ray absorption spectroscopy (XAS). This method was initially proposed by van der Laan and Thole,[28–30] who recognized that the intensity ratio of the "white-line" features observed in XAS measurements at the L_2 and L_3 absorption edges is directly proportional to the expectation value of the spin-orbit operator $\langle \mathrm{L} \cdot \mathrm{S} \rangle = \langle \sum_i l_i \cdot s_i \rangle$. As a result, XAS provides a direct probe of spin-orbit interactions, which is complementary to other techniques such as magnetic susceptibility, electron paramagnetic resonance, and Mossbauer spectroscopy (which probe spin-orbit coupling through the value of the Lande g-factor) or optical spectroscopy (which probes spin-orbit coupling through the observation of transitions forbidden by spin-only selection rules). This method was most recently employed by Laguna-Marco *et al.* to investigate spin-orbit coupling in $Ba_{1-x}Sr_xIrO_3$ ($x = 0$, 0.06, 0.12).[31] This study revealed a surprisingly large L_3/L_2 branching ratio, providing confirmation of the unusually strong spin-orbit interactions believed to be present in that compound.

In this paper, we report x-ray absorption spectroscopy (XAS) measurements on a series of iridium-based $5d$ compounds. In particular, we have carried out a comparative study of several topical iridates (Sr_2IrO_4, Na_2IrO_3, and $Y_2Ir_2O_7$) and several standard reference samples such as Ir, $IrCl_3$, and IrO_2. Our measurements reveal anomalously large branching ratios in all Ir-based compounds studied, and even (to a lesser extent) in elemental iridium itself. On the basis of these results, we propose that unusually strong spin-orbit coupling effects may be a common feature of all iridates, or at least all those possessing an octahedral local crystal field environment. To provide a point of comparison, similar measurements were also performed on a series of rhenium-based $5d$ compounds, including Re, ReO_2, Ba_2FeReO_6, and ReO_3. These compounds present a striking contrast to the iridates, displaying small, statistical branching ratios, which are consistent with negligible spin-orbit coupling effects.

II. EXPERIMENTAL DETAILS

X-ray absorption measurements were performed on a series of six iridium-based compounds, including Ir, $IrCl_3$, IrO_2, Na_2IrO_3, Sr_2IrO_4, and $Y_2Ir_2O_7$. These compounds encompass a wide range of physical properties, displaying a variety of electronic configurations ($5d^7$, $5d^6$, and $5d^5$), ionization states (Ir^0, Ir^{3+}, Ir^{4+}), transport properties (metallic, insulating), and crystal structures (cubic, tetragonal, orthorhombic, and monoclinic). However, one common feature shared by all of these compounds (with the exception of elemental Ir) is the presence of an octahedral local crystal field environment, wherein each Ir ion is surrounded by six nearest neighbor O or Cl ions. A more detailed description of the physical properties associated with these samples is provided in Table I. In order to provide a point of comparison, XAS measurements were also performed on a series of rhenium-based samples, including Re, ReO_2, Ba_2FeReO_6, and ReO_3. As in the case of the Ir-based samples, these Re-based compounds display a variety of different valence states (Re^0 [$5d^5$], Re^{4+} [$5d^3$], Re^{5+} [$5d^2$], Re^{6+} [$5d^1$]) and crystal structures, although all samples exhibit octahedral local coordination. Measurements were carried out on powder samples obtained from commercial suppliers (Ir, $IrCl_3$, IrO_2, Re, ReO_2, ReO_3) or prepared using conventional solid state reaction methods (Sr_2IrO_4, Na_2IrO_3, $Y_2Ir_2O_7$, Ba_2FeReO_6).[2,12,22,32] The purity of the commercial samples was quoted as 99.7% (ReO_2), 99.9% (ReO_3), 99.99% (Ir, $IrCl_3$, IrO_2), and 99.999% (Re) or higher. Thin, platelike, powder samples were prepared on sheets of Kapton tape, with two to three layers of sample used to minimize "pin-holing" effects and produce an average sample thickness of 5–10 μm (or ~2 absorption lengths).

X-ray absorption measurements were carried out using the hard x-ray microanalysis (HXMA) beamline 06ID-1 at the Canadian Light Source (CLS). Measurements were collected at both the L_2 ($2p_{1/2} \rightarrow 5d$) and L_3 ($2p_{3/2} \rightarrow 5d$) absorption edges, which occur at energies of 12.824 keV and 11.215 keV (Ir) and 11.959 keV and 10.535 keV (Re), respectively. The energy of the incident x-ray beam was selected using a Si(111) monochromator, with higher harmonic contributions suppressed by a combination of Rh-coated mirrors and a 50% detuning of the undulator. The size of the incident beam spot was approximately 0.4 mm × 3.8 mm. XAS measurements were performed in transmission geometry, using a series of three ion chambers (I_0, I_1, and I_2). The sample was mounted between I_0 and I_1, while a reference material (consisting of either elemental Ir or Re) was mounted between I_1 and I_2. This configuration allows a direct measurement of the linear x-ray attenuation coefficient, $\mu(E)$, which is defined by the intensity ratio of the incident and transmitted x-ray beams. In this case, $\mu_{\text{sample}}(E) = I_0/I_1$ and $\mu_{\text{ref}}(E) = I_1/I_2$. The energy calibration of this setup is accurate to within 0.25 eV, and direct comparisons between sample and reference spectra can be used to rule out any systematic energy drifts over the course of the experiment. All data sets were collected at room temperature.

TABLE I. Basic physical properties of the Ir and Re-based compounds studied in this experiment. Crystallographic and electronic data has been obtained from Refs. 5,6,15,16,21,22,32, and 51–57.

Compound	Electronic State	Electronics Properties	Crystal Structure	Ir Site Symmetry	Ir-O Distance (avg, min) [Å]	Ir-Ir Distance (min) [Å]
Ir	$5d^7$ (Ir)	Metallic	Cubic ($Fm\bar{3}m$)	$m\bar{3}m$	–	2.715
$IrCl_3$	$5d^6$ (Ir^{3+})	Insulating	Monoclinic ($C2/m$)	2	–	3.457
IrO_2	$5d^5$ (Ir^{4+})	Metallic	Orthorhombic ($P4_2/mnm$)	mmm	1.986, 1.960	3.159
Na_2IrO_3	$5d^5$ (Ir^{4+})	Insulating	Monoclinic ($C2/m$)	2	2.074, 2.060	3.138
Sr_2IrO_4	$5d^5$ (Ir^{4+})	Insulating	Tetragonal ($I4_1/acd$)	$\bar{1}$	2.006, 1.980	3.878
$Y_2Ir_2O_7$	$5d^5$ (Ir^{4+})	Insulating	Cubic ($Fd\bar{3}m$)	$.\bar{3}m$	2.015, 2.015	3.599
Compound	Electronic State	Electronic Properties	Crystal Structure	Re Site Symmetry	Re-O Distance (avg, min) [Å]	Re-Re Distance (min) [Å]
Re	$5d^5$ (Re)	Metallic	Hexagonal ($P6_3/mmc$)	$\bar{6}m2$	–	2.761
ReO_2	$5d^3$ (Re^{4+})	Metallic	Orthorhombic ($Pbcn$)	.2.	1.997, 1.941	2.614
Ba_2FeReO_6	$5d^2$ (Re^{5+})	Metallic	Cubic ($Fm\bar{3}m$)	$m\bar{3}m$	1.932, 1.932	5.717
ReO_3	$5d^1$ (Re^{6+})	Metallic	Cubic ($Pm\bar{3}m$)	$m\bar{3}m$	1.867, 1.867	3.734

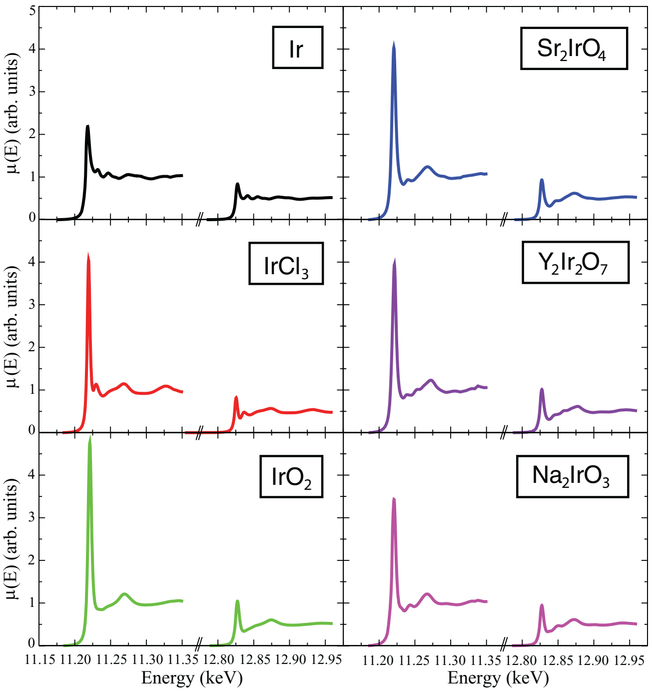

FIG. 1. (Color online) X-ray absorption spectra collected at the Ir L_3 (E = 11.215 keV) and L_2 (E = 12.824 keV) absorption edges for a series of Ir-based 5*d* compounds.

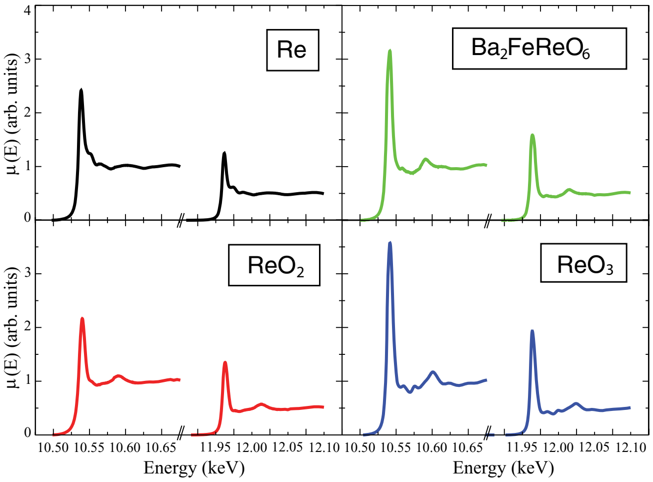

FIG. 2. (Color online) X-ray absorption spectra collected at the Re L_3 (E = 10.535 keV) and L_2 (E = 11.959 keV) absorption edges for a series of Re-based 5*d* compounds.

III. RESULTS AND DISCUSSION

X-ray absorption spectra collected at the Ir L_2 and L_3 absorption edges are provided in Fig. 1 for a series of Ir-based compounds. Each of these spectra can be decomposed into three main features: (i) a sharp, atomiclike "white-line" feature that corresponds to 2p → 5*d* electronic transitions, (ii) a steplike edge feature which is associated with 2p → continuum electronic excitations, and (iii) a series of smaller "fine structure" oscillations that arise from the backscattering of photoelectrons off of neighboring atoms. To enable accurate comparisons between compounds, μ(E) has been normalized such that the continuum step at the L_3 absorption edge is equal to unity for each sample. Accordingly, the continuum step at the L_2 absorption edge has been normalized to half this value.[33] This normalization scheme reflects the number of initial core-electron states available for the L_2 and L_3 absorption processes, since the ratio of occupied $2p_{1/2}$ and $2p_{3/2}$ states is 1:2.

The most striking characteristic of the XAS spectra shown in Fig. 1 are the prominent white-line features observed at both absorption edges. The integrated intensity (or area) of these white-line features is proportional to the local density of unoccupied final states in the system (i.e., the population of 5*d* holes).[34] Due to the selection rules that govern electric dipole transitions, the relative strength of the white-line features at the L_2 and L_3 edges (also known as the branching ratio) can be used to extract information about the total angular momentum J of the available 5*d* hole states. As ΔJ must be equal to 0 or ±1 for an allowed dipole transition, it follows that the L_2 edge will be exclusively sensitive to transitions involving $5d_{3/2}$ holes, while the L_3 edge will be sensitive to both $5d_{3/2}$ and $5d_{5/2}$. In the limit of negligible spin-orbit coupling effects, the $J = 3/2$ and $J = 5/2$ multiplets will be degenerate and the transition probabilities for L_2 and L_3 processes will only depend on the density of initial core-electron states. This yields the statistical branching ratio of $\mathrm{BR} = I_{L_3}/I_{L_2} = 2$, and an L_3 white line which is twice the size of the L_2 feature.[28–30]

The presence of strong white-line features indicates that there is a large local density of unoccupied 5*d* states in all of the Ir compounds measured in this study. As these white-line features are more pronounced at the L_3 edge than the L_2 edge, we can also infer that these unoccupied 5*d* states are primarily $5d_{5/2}$ rather than $5d_{3/2}$ in nature. Note that the ratio of white-line intensities is significantly smaller for pure iridium than for any of the Ir^{3+} or Ir^{4+} compounds. The absolute intensity of the L_3 white line is noticeably higher in the Ir^{3+} and Ir^{4+} compounds as well. Further from the absorption edge, differences in local chemical structure can be observed in the shape of the fine structure oscillations displayed by each compound.

Similar x-ray absorption spectra are shown for a series of Re-based compounds in Fig. 2. As in the spectra from the Ir-based compounds in Fig. 1, each of these samples displays a sharp white-line feature at the L_2 and L_3 absorption edges. The integrated intensity of the white-line features grows steadily with increasing oxidation state, as is expected given the rising number of 5*d* holes in the system. The ratio of the white-line intensities at the L_3 and L_2 edges appears to be considerably smaller than that of the Ir-based samples, and much closer to the statistical ratio expected in the absence of spin-orbit coupling effects. Furthermore, this ratio appears to be roughly equal for each of the Re-based compounds studied, in spite of the fact that the magnitude of the individual white-line features is changing quite significantly.

Several systematic effects can be observed by comparing spectra obtained for compounds with different valence states, such as Ir (Ir^0, $5d^7$), $IrCl_3$ (Ir^{3+}, $5d^6$), and IrO_2 (Ir^{4+}, $5d^5$). Representative XAS measurements for these three samples are provided in Fig. 3(a). Clearly, as the ionization state increases there are three significant changes in the XAS spectra at the L_3 edge: (1) The position of the white-line feature shifts towards higher energies. As described in Table II, the fitted peak center

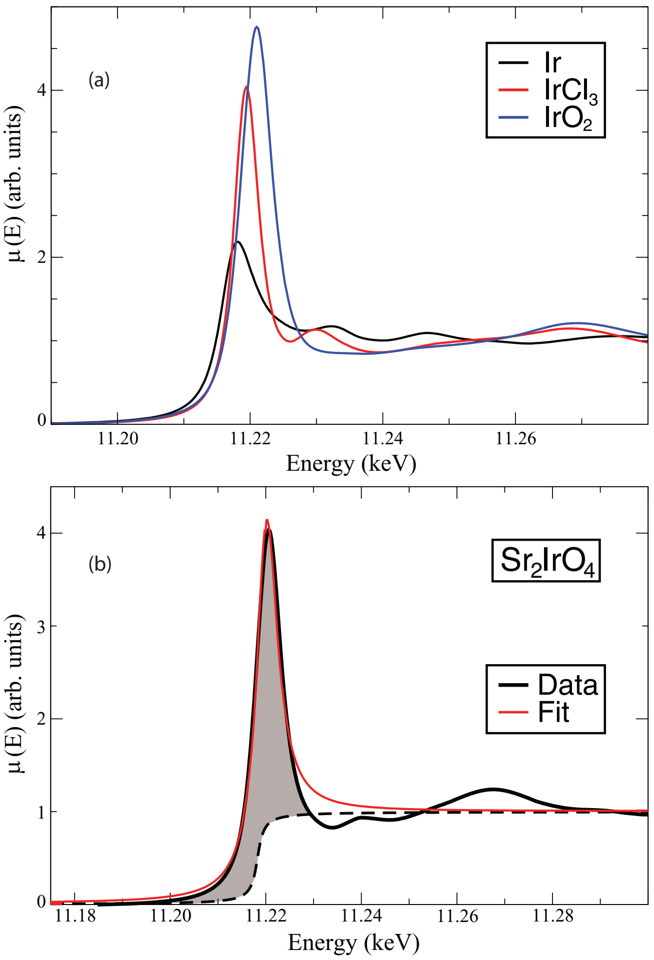

FIG. 3. (Color online) (a) A comparison of XAS specta at the Ir L_3 edge for Ir, IrCl$_3$, and IrO$_2$. (b) Experimental determination of the white-line intensity at the Ir L_3 absorption edge in Sr$_2$IrO$_4$. The solid black line represents the normalized x-ray attenuation coefficient μ(E), measured by XAS, while the dashed line represents the arctangent function used to model the continuum step at the L_3 absorption edge. The solid red line represents the best fit to the data using a Lorentzian + arctangent fit function.

shifts from 11218.1(1) eV to 11219.6(2) eV to 11220.7(1) eV following the progression from $5d^7$ to $5d^5$. This is a shift of ∼1.3 eV for each additional $5d$ hole. (2) The integrated intensity of the white-line feature monotonically increases, with fitted peak areas growing by a factor of ∼2 over the jump from $5d^7$ to $5d^5$. As discussed above, this effect can be understood in terms of the creation of $5d$ holes, which increase the number of accessible final states for $2p \rightarrow 5d$ electronic transitions. (3) The width of the white-line feature varies between oxidation states. This effect is not monotonic, but the FWHM of the white-line feature varies by ∼30–50% between different Ir valence states. The white line is sharpest in IrCl$_3$ (FWHM = 3.9(1) eV) and broadest in elemental Ir [FWHM = 6.6(2) eV]. This linewidth is related to the intrinsic bandwidth of the compound, but it is also influenced by broadening mechanisms such as the instrumental resolution, core-hole lifetime effects, and final-state lifetime effects.[34,35] These three observations are consistent with previous work by Choy *et al.*, who performed a systematic study of Ir L_3 line shapes in a series of Ir-based double perovskite compounds.[36] They can also be observed in our Re XAS spectra, following the progression from elemental Re (Re^0, $5d^5$) to ReO$_3$ (Re^{6+}, $5d^1$).

In order to discuss the spin-orbit coupling effects in these compounds on a quantitative level, it is necessary to accurately and precisely determine the intensity of the white-line features observed at the L_2 and L_3 absorption edges. The primary method used to obtain these white-line intensities is illustrated in Fig. 3(b), using a representative data set collected for Sr$_2$IrO$_4$ at the Ir L_3 edge. The experimental data is described by the solid black line. Here the continuum edge-step is modeled by an arctangent function, as shown by the dashed black line. This arctangent is centered at the absorption edge [taken as the inflection point on the rising edge of μ(E)] and is defined to have unit height. This function can be subtracted from the raw data, leaving only the contributions from the white-line feature (which is approximately Lorentzian in shape) and the fine structure oscillations present at higher energies. The integrated intensity of the white line is then calculated by numerically integrating the signal over the range of energies where it is positive valued [i.e., from below the edge to the

TABLE II. Summary of results obtained from XAS measurements on Ir and Re-based transition metal compounds. The intensity of the L_2 and L_3 white-line features (I_{L_2}, I_{L_3}), the branching ratio (BR = I_{L_3}/I_{L_2}), the spin-orbit expectation value ($\langle L \cdot S \rangle$), and the ratio of the $5d$ hole populations ($h_{5/2}/h_{3/2}$) have been determined by numeric integration. The branching ratio, peak position (E_{L_3}), and width (Γ_{L_3}) of the L_3 white-line feature have also been determined from fits to a Lorentzian + arctangent fit function.

Compound	Electronic State	$\langle n_h \rangle$	I_{L_3} (Numeric)	I_{L_2} (Numeric)	E_{L_3} (Fit) [eV]	Γ_{L_3} (Fit) [eV]	Branching Ratio (Numeric)	Branching Ratio (Fit)	$\langle L \cdot S \rangle$ [$\hbar^2$]	$\frac{h_{5/2}}{h_{3/2}}$
Ir	$5d^7$ (Ir)	3	14.3(6)	4.0(2)	11218.1(1)	6.6(1)	3.6(3)	3.2(1)	1.0(1)	2.7(2)
IrCl$_3$	$5d^6$ (Ir^{3+})	4	21.3(9)	3.0(1)	11219.6(2)	3.9(1)	7.1(6)	7.8(5)	2.5(1)	5.5(5)
IrO$_2$	$5d^5$ (Ir^{4+})	5	32(1)	4.7(2)	11220.7(1)	4.8(1)	6.9(6)	6.7(4)	3.1(1)	5.4(4)
Sr$_2$IrO$_4$	$5d^5$ (Ir^{4+})	5	30(1)	4.4(2)	11220.2(1)	5.5(1)	6.9(6)	7.0(4)	3.1(1)	5.4(4)
Y$_2$Ir$_2$O$_7$	$5d^5$ (Ir^{4+})	5	29(1)	5.1(2)	11220.0(2)	5.5(2)	5.8(5)	6.0(3)	2.8(2)	4.5(4)
Na$_2$IrO$_3$	$5d^5$ (Ir^{4+})	5	25(1)	4.5(2)	11220.1(2)	5.5(2)	5.5(4)	5.7(3)	2.7(2)	4.2(4)
Re	$5d^5$ (Re)	5	22.8(9)	10.3(4)	10538.2(1)	8.6(1)	2.2(2)	2.1(1)	0.3(3)	1.6(1)
ReO$_2$	$5d^3$ (Re^{4+})	7	19.0(8)	10.6(4)	10540.1(2)	9.0(3)	1.8(1)	1.8(1)	−0.5(4)	1.3(1)
Ba$_2$FeReO$_6$	$5d^2$ (Re^{5+})	8	29(1)	13.8(6)	10540.7(1)	7.7(2)	2.1(2)	2.1(1)	0.3(4)	1.5(1)
ReO$_3$	$5d^1$ (Re^{6+})	9	34(1)	16.7(7)	10541.3(2)	7.4(2)	2.0(2)	2.1(1)	0.1(5)	1.4(1)

point where μ(E) first intersects the arctangent function]. This yields the area of the shaded region in Fig. 3(b) which is shown in gray. This approach has the advantage of not being reliant on a particular choice of lineshape or fit function. This is important because the mixing of $5d$ and continuum states can result in broadening of the white line at higher energies, giving rise to an asymmetric Fano-type line shape rather than a pure Lorentzian.[38] The error bars for the integrated intensities are determined from the uncertainty in counting statistics ($\sigma \mathrm{I} = \sqrt{I}$) and the estimated uncertainty in the position of the arctangent function (which is allowed to vary by ±1eV). To provide a consistency check, each of the spectra was also fit using a simple Lorentzian + arctangent two-component fit function. The only fixed parameter in these fits was the amplitude of the arctangent function, which was set to unity in order to match the continuum edge step. The quality of these fits is illustrated by the solid red line in Fig. 3(b). Although the fit manages to capture the essential characteristics of the white-line feature (the position, the width, and the approximate area), it fails to account for the asymmetric line shape and the fine structure oscillations near the absorption edge. Within the limits of the experimental uncertainties, both the numeric integration and the fitting analysis produced the same results.

It is worth noting that in previous studies alternative methods have also been used to model the continuum edge step. In particular, absorption spectra from compounds such as Au or Pt, which have few $5d$ holes (and hence negligible white-line intensity), can be scaled, translated, and stretched to provide a relatively clean continuum background.[37,38] This approach has proven especially useful in cases where the observed white-line features are weak, as in compounds containing elements with nearly full $5d$ shells. For materials that exhibit strong white-line features, such as the Ir and Re-based compounds used in this study, we expect the difference between these two methods to have a negligible influence on the calculated branching ratios.

A list of the numerically integrated white-line intensities obtained for each compound can be found in Table II. The values of I_{L_2} and I_{L_3} have also been plotted graphically in Fig. 4(a). In the case of the four Re-based samples, both I_{L_2} and I_{L_3} increase approximately linearly with the average number of holes in the system, $\langle \mathrm{n}_h \rangle$. As discussed above, this is consistent with the increasing density of unoccupied $5d$ states that accompanies the introduction of additional holes. It is also clear that $\mathrm{I}_{L_3} \sim 2\mathrm{I}_{L_2}$, as one might expect to find in the absence of spin-orbit coupling effects. In the case of the Ir-based compounds, I_{L_3} appears to display the same linear dependence on $\langle \mathrm{n}_h \rangle$, while I_{L_2} remains approximately constant. A particularly interesting comparison can be made between elemental Re and the four Ir (IV) oxides, since all five of these compounds display the same $5d^5$ valence electron configuration. The Ir (IV) oxides are clearly distinguished by a simultaneous enhancement of the L_3 white-line feature and suppression of the L_2 white-line feature. However, the sum of the two white-line intensities ($\mathrm{I}_{L_2} + \mathrm{I}_{L_3}$) remains roughly constant for all five of the $5d^5$ samples.

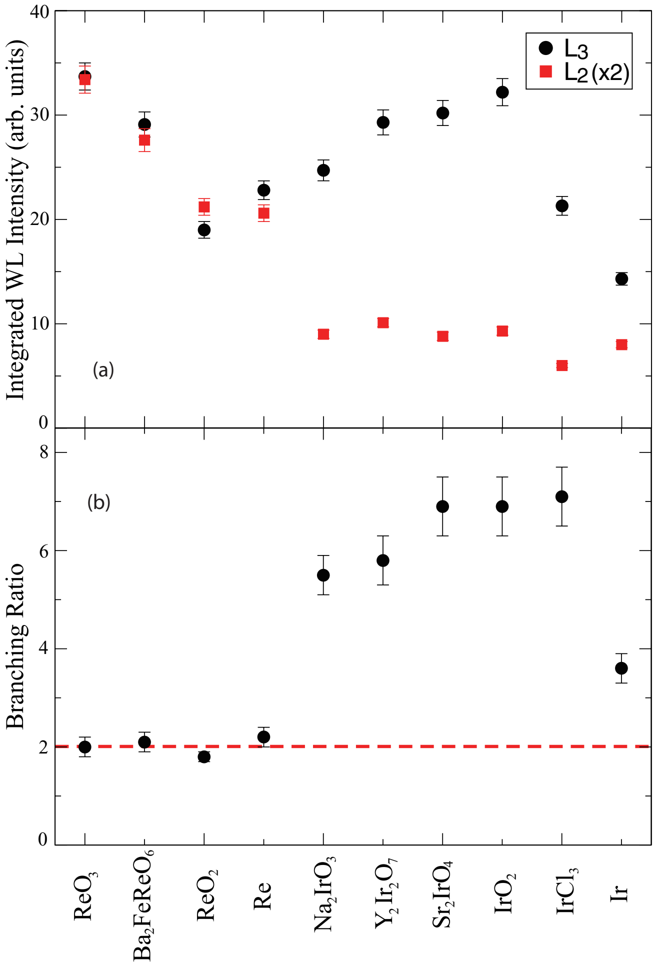

FIG. 4. (Color online) (a) Integrated intensity of the L_2 and L_3 white-line features in Ir and Re-based $5d$ transition metal compounds. All intensities were determined by numeric integration, as described in the main text. (b) Experimentally observed branching ratios, $\mathrm{I}_{L_3}/\mathrm{I}_{L_2}$, determined from the integrated intensities provided in (a). The dashed line represents the statistical branching ratio of $\mathrm{I}_{L_3}/\mathrm{I}_{L_2} = 2$ obtained in the limit of negligible spin-orbit coupling.

The values of the experimentally determined branching ratios are also provided in Table II, and are plotted graphically in Fig. 4(b). Here the branching ratio is defined as BR = $\mathrm{I}_{L_3}/\mathrm{I}_{L_2}$, where I_{L_n} is the integrated intensity of the white-line feature observed at a given absorption edge.[39] Using theoretical arguments proposed by van der Laan and Thole,[28–30] we can relate the branching ratio to the expectation value of the spin-orbit operator $\langle \mathbf{L} \cdot \mathbf{S} \rangle$: BR = $(2+\mathrm{r})/(1-\mathrm{r})$, where $\mathrm{r} = \langle \mathrm{L} \cdot \mathrm{S} \rangle / \langle \mathrm{n}_h \rangle$ and $\langle \mathrm{n}_h \rangle$ refers to the average number of $5d$ holes.[42] The value of $\langle \mathrm{L} \cdot \mathrm{S} \rangle$ is expressed in units of $\hbar^2$. It should be emphasized that the branching ratio is proportional to $\langle \mathrm{L} \cdot \mathrm{S} \rangle$ and not the spin-orbit interaction term in the Hamiltonian, $H_{\mathrm{SO}} = \zeta_{5d} \mathbf{L} \cdot \mathbf{S}$. While a large $\langle \mathrm{L} \cdot \mathrm{S} \rangle$ does imply the presence of strong spin-orbit coupling effects, the converse is not necessarily true. In the event that the spin or orbital moments in the system are quenched, it is possible to have $\langle \mathrm{L} \cdot \mathrm{S} \rangle \sim 0$ even if significant spin-orbit interactions are present. Similarly, if the electronic bandwidth is large compared to the strength of the spin-orbit coupling, overlap between the $J = 3/2$ and $J = 5/2$ levels can result in an approximately statistical branching ratio and a significantly reduced $\langle \mathrm{L} \cdot \mathrm{S} \rangle$.

Note that we observe anomalously high branching ratios in all of the Ir-based compounds measured in this study, including $IrCl_3$, IrO_2, Na_2IrO_3, Sr_2IrO_4, and $Y_2Ir_2O_7$. These experimental values are over several times larger than the statistical branching ratio (BR = 2), indicating the presence of extremely large spin-orbit coupling effects. While this result may not be particularly surprising in the context of Sr_2IrO_4, Na_2IrO_3, and $Y_2Ir_2O_7$ (since each of these samples has previously been associated with unconventional spin-orbit-induced ground states), it is quite unexpected in the case of the IrO_2 and $IrCl_3$ reference samples. Interestingly, the observed branching ratios do not appear to vary significantly between these compounds. While the ratios observed for Sr_2IrO_4 and IrO_2 appear to be slightly higher, and those for Na_2IrO_3 and $Y_2Ir_2O_7$ appear to be slightly lower, these variations do not seem to be correlated with any basic structural properties, such as space group, site symmetry, or local bond length (a full comparison of these properties can be found in Tables I and II). Perhaps most surprisingly, the branching ratio shows almost no dependence on Ir oxidation state (Ir^{3+} or Ir^{4+}) or choice of anion (O or Cl). This is clearly demonstrated by the $IrCl_3$ data, which is almost indistinguishable from the iridium (IV) oxides. In contrast, the branching ratios observed for elemental Ir and the four Re-based samples are dramatically different. Elemental Ir displays a branching ratio of BR = 3.2–3.6, indicating the presence of a moderate spin-orbit enhancement, but significantly less than in any of the other Ir-based compounds studied. The four Re-based compounds display branching ratios of ∼2, which is approximately equal to the value of the statistical branching ratio. This suggests that either the spin-orbit coupling effects in these Re-based transition metal oxides are negligible, or that a combination of bandwidth effects and quenching of orbital momentum results in an extremely small expectation value for the spin-orbit operator $\mathrm{L}\cdot\mathrm{S}$. While the latter is certainly a possibility, it would appear to be inconsistent with x-ray magnetic circular dichroism (XMCD) measurements on Ba_2FeReO_6[43] which indicate that the Re moments are unquenched.

This branching ratio data can also be used to extract information regarding the relative $5d$-hole populations of the $J = 3/2$ and $J = 5/2$ manifolds. The ratio of $J = 5/2$ and $J = 3/2$ hole populations, $h_{5/2}/h_{3/2}$, can be determined from the expression $\mathrm{BR} = K[1 + 6(h_{5/2}/h_{3/2})]$, where K is a multiplicative constant which contains the transition-matrix elements corresponding to the L_2 and L_3 absorption processes.[38,40] In the limit of negligible spin-orbit coupling, the $J = 5/2$ and $J = 3/2$ levels will be degenerate and $h_{5/2}/h_{3/2}$ will display a statistical value of 1.5. Following the approach of Qi *et al.*,[38] the statistical branching ratios observed in the four Re-based compounds can be used to determine an empirical value of $K = 0.8$ for the transition-matrix scale factor. This allows an experimental value of $h_{5/2}/h_{3/2}$ to be calculated for each sample, as displayed in Table II. The large values of $h_{5/2}/h_{3/2}$ observed for the Ir-based compounds in this study indicate a strong preference for the $5d$ valence electrons to occupy states with $J = 3/2$ rather than $J = 5/2$. In the case of $IrCl_3$ and the iridium oxides, the population of unoccupied $J = 5/2$ holes is approximately five times higher than that of the $J = 3/2$ holes.

It is interesting to compare these results to the previously reported branching ratios in the literature. As noted in the introduction, recent XAS measurements by Laguna-Marco and collaborators[31] have revealed an anomalously large branching ratio in the layered iridate $Ba_{1-x}Sr_xIrO_3$ ($x = 0$, 0.06, 0.12). The branching ratio quoted in this study is BR ∼ 4, a value which is somewhat smaller than the ratios reported in this study, but is still equal to twice the statistical branching ratio. Similar results have also been reported by Boseggia *et al.*,[44] who performed resonant magnetic x-ray scattering measurements on the bilayer iridate $Sr_3Ir_2O_7$. The XAS measurements in this study suggest a BR ∼ 5, in very good agreement with the results reported here. Previous measurements on elemental iridium also reveal slightly enhanced branching ratios, ranging from BR ∼ 2.4[37] to ∼4.0.[38] Our value of BR = 3.2–3.6 falls well within this range. Somewhat surprisingly, XAS measurements on binary iridium compounds (IrAl, $IrAl_3$, IrSi, and $IrSi_3$),[37] iridium alloys,[45,46] and Ir-Fe multilayers[47] are all consistent with approximately statistical branching ratios (BR ∼ 2). This suggests that there must be some property unique to the iridium oxides and chlorides that results in a natural tendency towards large spin-orbit coupling effects. The observation of enhanced branching ratios in late $5d$ transition metal oxides such as IrO_2, PtO_2, and Au_2O_3, has previously been attributed to a combination of charge transfer and crystal electric field effects.[40] As in the case of our Re-based samples, XAS measurements performed on early $5d$ transition metals (Os, W, Ta)[38,40] and their associated oxides (OsO_2, WO_2, and Ta_2O_5)[40] all yield branching ratios of ∼2. A similar trend is observed in compounds containing lighter $4d$ elements, such as Ru (RuO_2, Sr_2RuO_4, $Sr_4Ru_2O_9$, $Ca_{1-x}Sr_xRuO_3$)[48,49] and Rh (Ca_3CoRhO_6, Ca_3FeRhO_6),[50] which consistently reveal small, statistical branching ratios.

The value of $\langle \mathrm{L}\cdot\mathrm{S}\rangle$ can also be compared to previously reported spin-orbit interaction strengths in the literature. Applying a combination of XAS measurements and configuration interaction calculations, Laguna-Marco *et al.* determined that the expectation value of $\langle \mathrm{L}\cdot\mathrm{S}\rangle \sim 2$ in $Ba_{1-x}Sr_xIrO_3$ corresponds to a spin-orbit coupling coefficient of ζ_{5d} ∼0.3 eV.[31] Although such calculations are beyond the scope of the present study, we note that the coupling coefficient for Sr_2IrO_4 has been determined to be $\zeta_{5d} \sim 0.5$ eV from optical conductivity measurements.[1] Given the expectation value of $\langle \mathrm{L}\cdot\mathrm{S}\rangle = 3.1 \pm 0.1$ determined for Sr_2IrO_4 from our Ir XAS measurements, there appears to be a relatively simple scaling relation between ζ_{5d} and $\langle \mathrm{L}\cdot\mathrm{S}\rangle$ (i.e., $\zeta_{5d} \sim 0.15\langle \mathrm{L}\cdot\mathrm{S}\rangle$). Based on this relation, we predict ζ_{5d} will be ∼0.5 eV for IrO_2, and ∼0.4 eV for $IrCl_3$, Na_2IrO_3 and $Y_2Ir_2O_7$.

These results are also relevant to the $j_{\mathrm{eff}} = 1/2$ model which has been put forward to explain the insulating properties of iridates such as Sr_2IrO_4 and Na_2IrO_3.[1,2] In the $j_{\mathrm{eff}} = 1/2$ picture, a combination of strong $5d$ spin-orbit coupling effects and a large octahedral crystal field acts to split the degeneracy of the $5d$ electronic orbitals, creating a low-lying $j_{\mathrm{eff}} = 3/2$ multiplet (with 4-fold degeneracy) and a higher $j_{\mathrm{eff}} = 1/2$ multiplet (with twofold degeneracy). This process can be regarded from two alternative (although ultimately equivalent) viewpoints:

(1) As arising from the action of $5d$ spin-orbit coupling on the lower t_{2g} and upper e_g manifolds created by strong crystal field splitting. In this case, the $j_{\mathrm{eff}} = 1/2$ and 3/2 states are both derived from the lower-lying t_{2g} levels.

(2) As arising from the action of the octahedral crystal field on the lower $J = 3/2$ and upper $J = 5/2$ manifolds created by strong 5*d* spin-orbit coupling effects. In this case, the $j_{\text{eff}} = 3/2$ states are derived from the lower-lying $J = 3/2$ levels and the $j_{\text{eff}} = 1/2$ states are split off from the upper $J = 5/2$ levels.

For an Ir^{4+} ion with a $5d^5$ electronic configuration (as in Sr_2IrO_4 and Na_2IrO_3), the lowest-lying $j_{\text{eff}} = 3/2$ states will be fully occupied, and the $j_{\text{eff}} = 1/2$ band will be partially occupied by a single electron. At this point, even relatively weak 5*d* electronic correlations can split the narrow $j_{\text{eff}} = 1/2$ band into an upper Hubbard band and a lower Hubbard band, leading to the development of an insulating gap.[1] One of the chief methods of distinguishing the $j_{\text{eff}} = 1/2$ ground state from a conventional low spin $S = 1/2$ state (as produced by large crystal field effects in the absence of strong spin-orbit coupling) is by comparing the ratio of the transition probabilities at the L_2 and L_3 edges.[2] In the $S = 1/2$ scenario, the lowest unoccupied state will be found in the t_{2g} manifold, which possesses mixed $J = 3/2$ and $J = 5/2$ character. As a result, both L_2 ($2p_{1/2} \rightarrow 5d_{3/2}$) and L_3 ($2p_{3/2} \rightarrow 5d_{3/2,5/2}$) transitions will be allowed processes. In the $j_{\text{eff}} = 1/2$ scenario, the $j_{\text{eff}} = 3/2$ band derived from the $J = 3/2$ states will be completely occupied, effectively prohibiting any transitions at the L_2 edge. This dramatic difference in transition probabilities should be reflected in the relative strength of the L_2 and L_3 white-line features, giving rise to the type of strongly enhanced branching ratios observed in this study.

The first experimental signature of the $j_{\text{eff}} = 1/2$ ground state was reported by Kim *et al.*, who observed the characteristic difference in L_2 and L_3 transition probabilities using resonant magnetic x-ray scattering measurements on Sr_2IrO_4.[2] The interpretation of these results was subsequently called into question by Chapon and Lovesey,[41] who proposed an alternative Ir ground state wave function involving a superposition of conjugate states in a Kramers doublet. This alternative wave function was calculated to have a relatively small branching ratio of $\text{BR} = 1.74$.[41] The results of the present study, which determine the branching ratio of Sr_2IrO_4 to be 6.9 ± 0.6, are clearly inconsistent with this theoretical prediction.[58]

IV. CONCLUSIONS

In conclusion, we have used x-ray absorption spectroscopy techniques to investigate spin-orbit coupling effects in a series of Ir and Re-based 5*d* compounds. We observe anomalously large L_3/L_2 branching ratios in all Ir-based compounds measured in this study, up to several times larger than the statistical branching ratio of $I_{L_3}/I_{L_2} = 2$. These enhanced branching ratios indicate that the expectation value for the spin-orbit operator, $\langle \mathbf{L} \cdot \mathbf{S} \rangle$, is very large in these systems, reflecting the presence of strong 5*d* spin-orbit coupling effects. This observation is consistent with recent proposals for novel spin-orbit-induced physics in iridates such as Sr_2IrO_4,[1,2,10] Na_2IrO_3,[17,18] and $Y_2Ir_2O_7$.[23–27] Surprisingly, the size of the observed branching ratios does not appear to be sensitive to the detailed structural or electronic properties of these systems. The sole exception to this rule appears to be provided by elemental iridium, which exhibits a much more modest spin-orbit enhancement, and a branching ratio significantly closer to the statistical value. The one common feature shared by all of these compounds (save for Ir itself) appears to be the presence of an octahedral crystal field environment. These anomalously large branching ratios are not common to all 5*d* compounds, as demonstrated by XAS measurements on a series of Re-based transition metal oxides. Measurements on these Re-based samples reveal small, statistical branching ratios, a result which implies the presence of minimal spin-orbit coupling effects.

On the basis of these measurements, we propose that even the physics of simple iridium compounds, such as IrO_2 and $IrCl_3$, may warrant further investigation due to the presence of unusually large spin-orbit coupling effects. It may also be productive to extend these studies to include Ir-based compounds which exhibit higher oxidation states (such as Ir^{5+} or Ir^{6+}), or which display tetrahedral rather than octahedral local coordination. In this regard, there appears to be a particularly strong case for complementary studies involving XMCD measurements, similar to those reported in Ref. 31. We hope these results will help to guide and inform future studies of these novel electronic and magnetic systems.

ACKNOWLEDGMENTS

We would like to acknowledge useful discussions with Hlynur Gretarsson and Arun Paramekanti, and assistance in sample preparation from Andreea Lupascu and Zixin Nie. Elements of the data reduction and analysis for this experiment were performed using the Athena software package created by Bruce Ravel. Work at the University of Toronto was supported by NSERC of Canada, the Banting Postdoctoral Fellowship program, and the Canada Research Chair program. Use of the HXMA beamline at the CLS is supported by NSERC of Canada, NRC of Canada, CIHR, and the University of Saskatchewan.

---

[1] B. J. Kim, H. Jin, S. J. Moon, J.-Y. Kim, B.-G. Park, C. S. Leem, J. Yu, T. W. Noh, C. Kim, S.-J. Oh, J.-H. Park, V. Durairaj, G. Cao, and E. Rotenberg, Phys. Rev. Lett. **101**, 076402 (2008).

[2] B. J. Kim, H. Ohsumi, T. Komesu, S. Sakai, T. Morita, H. Takagi, and T. Arima, Science **323**, 1329 (2009).

[3] S. J. Moon, H. Jin, K. W. Kim, W. S. Choi, Y. S. Lee, J. Yu, G. Cao, A. Sumi, H. Funakubo, C. Bernhard, and T. W. Noh, Phys. Rev. Lett. **101**, 226402 (2008).

[4] G. Cao, J. Bolivar, S. McCall, J. E. Crow, and R. P. Guertin, Phys. Rev. B **57**, R11039 (1998).

[5] M. K. Crawford, M. A. Subramanian, R. L. Harlow, J. A. Fernandez-Baca, Z. R. Wang, and D. C. Johnston, Phys. Rev. B **49**, 9198 (1994).

[6] Q. Huang, J. L. Soubeyroux, O. Chmaissem, I. Natali Sora, A. Santoro, R. J. Cava, J. J. Krajewski, and W. F. Peck, Jr., J. Solid State Chem. **112**, 355 (1994).

[7] M. Ge, T. F. Qi, O. B. Korneta, D. E. De Long, P. Schlottmann, W. P. Crummett, and G. Cao, Phys. Rev. B **84**, 100402 (2011).

[8] S. Chikara, O. Korneta, W. P. Crummett, L. E. DeLong, P. Schlottmann, and G. Cao, Phys. Rev. B **80**, 140407 (2009).

[9] J. H. Kim, D. Casa, M. H. Upton, T. Gog, Y.-J. Kim, J. F. Mitchell, M. van Veenendaal, M. Daghofer, J. van den Brink, G. Khaliullin, and B. J. Kim, Phys. Rev. Lett. **108**, 177003 (2012).

[10] G. Jackeli and G. Khaliullin, Phys. Rev. Lett. **102**, 017205 (2009).

[11] G. Cao, Y. Xin, C. S. Alexander, J. E. Crow, P. Schlottmann, M. K. Crawford, R. L. Harlow, and W. Marshall, Phys. Rev. B **66**, 214412 (2002).

[12] Y. Singh and P. Gegenwart, Phys. Rev. B **82**, 064412 (2010).

[13] X. Liu, T. Berlijn, W.-G. Yin, W. Ku, A. Tsvelik, Y.-J. Kim, H. Gretarsson, Y. Singh, P. Gegenwart, and J. P. Hill, Phys. Rev. B **83**, 220403(R) (2011).

[14] Y. Singh, S. Manni, J. Reuther, T. Berlijn, R. Thomale, W. Ku, S. Trebst, and P. Gegenwart, Phys. Rev. Lett. **108**, 127203 (2012).

[15] S. K. Choi, R. Coldea, A. N. Kolmogorov, T. Lancaster, I. I. Mazin, S. J. Blundell, P. G. Radaelli, Y. Singh, P. Gegenwart, K. R. Choi, S.-W. Cheong, P. J. Baker, C. Stock, and J. Taylor, Phys. Rev. Lett. **108**, 127204 (2012).

[16] F. Ye, S. Chi, H. Cao, B. C. Chakoumakos, J. A. Fernandez-Baca, R. Custelcean, T. F. Qi, O. B. Korneta, and G. Cao, Phys. Rev. B **85**, 180403(R) (2012).

[17] J. Chaloupka, G. Jackeli, and G. Khaliullin, Phys. Rev. Lett. **105**, 027204 (2010).

[18] A. Shitade, H. Katsura, J. Kunes, X.-L. Qi, S.-C. Zhang, and N. Nagaosa, Phys. Rev. Lett. **102**, 256403 (2009).

[19] S. Nakatsuji, Y. Machida, Y. Maeno, T. Tayama, T. Sakakibara, J. van Duijn, L. Balicas, J. N. Millican, R. T. Macaluso, and J. Y. Chan, Phys. Rev. Lett. **96**, 087204 (2006).

[20] Y. Machida, S. Nakatsuji, S. Onoda, T. Tayama, and T. Sakakibara, Nature (London) **463**, 210 (2010).

[21] D. Yanagishima and Y. Maeno, J. Phys. Soc. Jpn. **70**, 2880 (2001).

[22] N. Taira, M. Wakeshima, and Y. Hinatsu, J. Phys.: Condens. Matter **13**, 5527 (2001).

[23] D. A. Pesin and L. Balents, Nat. Phys. **6**, 376 (2010).

[24] B.-J. Yang and Y. B. Kim, Phys. Rev. B **82**, 085111 (2010).

[25] M. Kargarian, J. Wen, and G. A. Fiete, Phys. Rev. B **83**, 165112 (2011).

[26] X. Wan, A. M. Turner, A. Vishwanath, and S. Y. Savrasov, Phys. Rev. B **83**, 205101 (2011).

[27] W. Witczak-Krempa and Y. B. Kim, Phys. Rev. B **85**, 045124 (2012).

[28] G. van der Laan and B. T. Thole, Phys. Rev. Lett. **60**, 1977 (1988).

[29] B. T. Thole and G. van der Laan, Phys. Rev. B **38**, 3158 (1988).

[30] B. T. Thole and G. van der Laan, Phys. Rev. A **38**, 1943 (1988).

[31] M. A. Laguna-Marco, D. Haskel, N. Souza-Neto, J. C. Lang, V. V. Krishnamurthy, S. Chikara, G. Cao, and M. van Veenendaal, Phys. Rev. Lett. **105**, 216407 (2010).

[32] B. C. Jeon, C. H. Kim, S. J. Moon, W. S. Choi, H. Jeong, Y. S. Lee, J. Yu, C. J. Won, J. H. Jung, N. Hur, and T. W. Noh, J. Phys.: Condens. Matter **22**, 345602 (2010).

[33] It should be noted that this normalization results in relatively minor changes to the experimental data. The average correction to $\mu(E)$ at the L_2 edge is on the order of 11%, and serves to reduce, rather than enhance, the observed branching ratio in all cases.

[34] T. K. Sham, Phys. Rev. B **31**, 1888 (1985).

[35] R. D. Leapman, L. A. Grunes, and P. L. Fejes, Phys. Rev. B **26**, 614 (1982).

[36] J.-H. Choy, D.-K. Kim, S.-H. Hwang, G. Demazeau, and D.-Y. Jung, J. Am. Chem. Soc. **117**, 8557 (1995).

[37] Y. Jeon, B. Qi, F. Lu, and M. Croft, Phys. Rev. B **40**, 1538 (1989).

[38] B. Qi, I. Perez, P. H. Ansari, F. Lu, and M. Croft, Phys. Rev. B **36**, 2972 (1987).

[39] Note that we have elected to follow the convention of recent work (Refs. 31, 40, and 41) in using a direct ratio of $\mathrm{BR} = \mathrm{I}_{L_3}/\mathrm{I}_{L_2}$, rather than the original fractional ratio of $\mathrm{BR} = \mathrm{I}_{L_3}/(\mathrm{I}_{L_2} + \mathrm{I}_{L_3})$ employed in Refs. 28–30.

[40] D.-Y. Cho, J. Park, J. Yu, and J.-G. Park, J. Phys.: Condens. Matter **24**, 055503 (2012).

[41] L. C. Chapon and S. W. Lovesey, J. Phys.: Condens. Matter **23**, 252201 (2011).

[42] Two alternative forms of this relation can be found in the literature, depending on whether the summation in $\langle \mathrm{L} \cdot \mathrm{S} \rangle = \langle \sum_i l_i \cdot s_i \rangle$ is performed over occupied or unoccupied $5d$ states. The two relations differ solely by a change of sign, such that $\mathrm{BR} = (2+\mathrm{r})/(1-\mathrm{r})$ using the unoccupied/$5d$ hole convention and $\mathrm{BR} = (2-\mathrm{r})/(1+\mathrm{r})$ using the occupied/$5d$ electron convention. We have adopted the former convention to remain consistent with previous discussion of branching ratios in Ir-based systems (Refs. 31 and 41).

[43] A. Sikora, C. Kapusta, M. Borowiec, C. J. Oates, V. Prochazka, D. Rybicki, D. Zajac, J. M. De Teresa, C. Marquina, and M. R. Ibarra, Appl. Phys. Lett. **89**, 062509 (2006).

[44] S. Boseggia, R. Springell, H. C. Walker, A. T. Boothroyd, D. Prabhakaran, D. Wermeille, L. Bouchenoire, S. P. Collins, and D. F. McMorrow, Phys. Rev. B **85**, 184432 (2012).

[45] G. Schutz, R. Wienke, W. Wilhelm, W. Wagner, P. Kienle, R. Zeller, and R. Frahm, Z. Phys. B **75**, 495 (1989).

[46] V. V. Krishnamurthy, M. Suzuki, N. Kawamura, T. Ishikawa, and Y. Kohori, Hyperfine Interact. **136/137**, 361 (2001).

[47] F. Wilhelm, P. Poulopoulos, H. Wende, A. Scherz, K. Baberschke, M. Angelakeris, N. K. Flevaris, and A. Rogalev, Phys. Rev. Lett. **87**, 207202 (2001).

[48] Z. Hu, H. von Lips, M. S. Golden, J. Fink, G. Kaindl, F. M. F. de Groot, S. Ebbinghaus, and A. Reller, Phys. Rev. B **61**, 5262 (2000).

[49] J. Okamoto, T. Okane, Y. Saitoh, K. Terai, S.-I. Fujimori, Y. Muramatsu, K. Yoshii, K. Mamiya, T. Koide, A. Fujimori, Z. Fang, Y. Takeda, and M. Takano, Phys. Rev. B **76**, 184441 (2007).

[50] T. Burnus, Z. Hu, H. Wu, J. C. Cezar, S. Niitaka, H. Takagi, C. F. Chang, N. B. Brookes, H.-J. Lin, L. Y. Jang, A. Tanaka, K. S. Liang, C. T. Chen, and L. H. Tjeng, Phys. Rev. B **77**, 205111 (2008).

[51] R. W. G. Wyckoff, *Crystal Structures*, Vol. 1 (Wiley, New York, 1963).

[52] K. Brodersen, F. Moers, and H. G. Schnering, Naturwissenschaften **52**, 205 (1965).

[53] D. Babel and P. Deigner, Z. Anorg. Allg. Chem. **339**, 57 (1965).

[54] A. A. Bolzan, C. Fong, B. J. Kennedy, and C. J. Howard, Acta Crystallogr. Sect. B **53**, 373 (1997).

[55] K. Meisel, Z. Anorg. Allg. Chem. **207**, 107 (1932).

[56] A. Magneli, Acta Crystallogr. **9**, 1038 (1956).

[57] J. Gopalakrishnan, A. Chattopadhyay, S. B. Ogale, T. Venkatesan, R. L. Greene, A. J. Millis, K. Ramesha, B. Hannoyer, and G. Marest, Phys. Rev. B **62**, 9538 (2000).

[58] Following the initial submission of this manuscript, this result has also been confirmed by independent XAS/XMCD studies on $\mathrm{Sr_2IrO_4}$ [see D. Haskel *et al.*, Phys. Rev. Lett. **109**, 027204 (2012)].